Tech Science Press

Preparation of Cellulose Nanofibrils by Multi-Site Regioselective Oxidation

Liying Song[1], Xixiang Pei[2], Rui Li[1], Haitao Chen[1,*] and Xiaozheng Sun[1,*]

[1]College of Engineering, Northeast Agricultural University, Harbin, 150030, China
[2]Harbin Botai Biological Technology Co., Ltd., Harbin, 150030, China
*Corresponding Authors: Haitao Chen. Email: htchen@neau.edu.cn; Xiaozheng Sun. Email: sxz1976@hotmail.com

Abstract: Cellulose nanofibrils (CNFs) are promising sustainable materials that can be applied to nanocomposites, as well as medical and life-sciences devices. However, methods for the preparation of these important materials are energy intensive because heating and mechanical disintegration are required to produce cellulose fibers below 100 nm in size. In this study, CNFs were prepared through the multi-site regioselective oxidation of cellulose with 2,2,6,6-tetramethylpiperidine-1-oxyl (TEMPO) and periodate at room temperature (20–25°C), without any mechanical-disintegration treatment. Transmission electron microscopy (TEM) revealed that the CNFs had the average widths of 14.1, 55.4, and 81.9 nm for three different treatments. Fourier-transform infrared spectroscopy revealed that carboxyl groups were created on the surfaces of the microfibrils, while X-ray diffraction studies showed that the cellulose I structure was maintained after oxidation, and that the cellulose nanofibril crystallinity index exceeded 70%. These results demonstrate that CNFs can be prepared by multi-site regioselective oxidation at room temperature in the absence of mechanical disintegration. In addition, a model was developed to calculate the total content of carboxylate and aldehyde groups of CNFs prepared by the TEMPO mediate oxidation, the periodate oxidation, and the multi-site regioselective oxidation methods based on the particle width determined by TEM. The calculated values of the model were in good agreement with the total content (experimental value) of carboxylate and aldehyde groups of CNFs prepared by the TEMPO-mediated oxidation and the multi-site regioselective oxidation methods. However, the model was not valid for CNFs prepared by the periodate oxidation method.

Keywords: Cellulose nanofibril; multi-site regioselective oxidation; total content of carboxylate and aldehyde groups; particle width

1 Introduction

Nanocelluloses, which encompass a range of cellulosic materials with at least one dimension in the range 1–100 nm, are promising materials in the fields of sustainable materials and nanocomposites, as well as for use in medical and life-sciences devices [1,2] due to their impressive mechanical properties, reinforcing capabilities, abundance, low densities, and biodegradabilities [3]. Therefore, nanocelluloses have attracted

significant interest over the past few decades, and are expected to play essential roles in the development of next-generation high-tech nanomaterials.

Nanocelluloses are generally categorized into three main types: cellulose nanofibrils (CNFs, also known as nanofibrillated cellulose), cellulose nanocrystals (CNCs, also referred to nanocrystalline cellulose or cellulose nanowhiskers), and bacterial nanocelluloses (BNCs, also known as microbial nanocelluloses) [1]. To date, two types of method have been used to prepare nanocelluloses, namely the "top-down" approach that involves enzymatic/chemical/physical methodologies for the isolation of nanocelluloses from wood and forest/agricultural residues, and the "bottom-up" bacterial preparation of nanocelluloses from glucose. Top-down methods are more commonly used since cellulose, the main constituent of plant cell walls, is the most abundant organic substance on Earth [4]; it is also renewable, biodegradable, and non-toxic [3]. However, cellulose fibers are not easy to disintegrate into nanocelluloses due to the large numbers of hydroxyl groups on the cellulose chains that are strongly hydrogen bonded [5].

CNFs can be prepared by microfluidization [6,7], grinding [8], homogenization [9] and ultrasonication [9]. Since neighboring elementary fibrils are either chemically cross-linked [5] or physically entangled by single-chain polysaccharides [10], intense energy is required to disintegrate these bundles of elementary fibrils [11]. CNCs are most commonly prepared by sulfuric acid hydrolysis [12]. The use of sulfuric acid generates acidic sulfate ester groups (OSO_3^-) on the nanofibril surfaces, resulting in electrostatic repulsion between the rod-like colloidal particles and the formation of stable aqueous suspensions.

Increasing the content of functional groups on the surface of cellulose microfibrils can promote nanofibrillation and increase the yield of nanocelluloses [13–15]. The isolation of nanocelluloses can almost be achieved in the absence of mechanical energy when the charged content on the surface surpasses a threshold of around 3 mmol/g [11]. The surface of microfibrils treated by sulfuric acid hydrolysis has an OSO_3^- content not exceeding 0.4 mmol/g, and usually requires ultrasonic treatment to obtain CNCs [12,16]. The maximum carboxylate content that can be introduced by means of TEMPO-mediated oxidation is around 2.0 mmol/g when the TEMPO/NaBr/NaClO system is used [17,18]. After pretreatment by TEMPO mediated oxidation, a mechanical nanofibrillation process is required to prepare CNFs with a width of 4 nm [13,14].

Cellulose has three reactive hydroxyl groups in its repeat unit, one primary and two secondary hydroxyl groups. The total oxidation of these three hydroxyl groups is an efficient way to increase the number of charged groups on the surfaces of nanocelluloses. There are two main methods to oxidize selectivly the reactive hydroxyl groups of cellulose. One approach is the TEMPO-mediated oxidation of the primary hydroxyl groups at C6 of the cellulose repeat units [13,14,17], while the other approach involves the periodate oxidation of the two secondary hydroxyl groups, with cleavage of the C2–C3 bond in the glucose repeat units and the formation of two aldehyde groups per glucopyranose unit [11,15]. Much research has been conducted to prepare nanocelluloses using these two approaches separately. However, to the best of our knowledge, no research has been conducted into the preparation of CNFs that combines the two most common selective oxidation processes, namely concurrent oxidation with TEMPO and periodate. We developed a method for preparing CNFs by concurrent oxidation with TEMPO and periodate, and defined as multi-site regioselective oxidation method [19].

In addition, the carboxylate and aldehyde groups on the surface of CNFs have an important influence on the yield, chemical, and physical properties of CNFs [11,15,17]. Therefore, the carboxyl and aldehyde groups on the surface of CNFs are usually investigated in the studies on CNFs. Since the particle width of CNFs is easy to investigate through the transmission electron microscope (TEM) image and the TEM-image-processing software. So a suitable model used to calculate the total content of carboxylate and aldehyde groups on the surface of CNFs based on the particle width will help the expert to easier know the oxidation level of cellulose.

The objective of this study was to determine whether or not CNFs can be prepared by the multi-site regioselective oxidation process at room temperature without the requirement of any mechanical disintegration. In this work, CNFs were prepared for the first time by the multi-site regioselective oxidation of cellulose with TEMPO and periodate at room temperature without any mechanical treatment. The CNFs prepared in this manner were characterized by FTIR, XRD, and TEM. In addition, a model was developed to calculate the total content of carboxylate and aldehyde groups of CNFs prepared by the TEMPO mediate oxidation, the periodate oxidation and the multi-site regioselective oxidation methods based on the particle width of CNFs. The model with the correlation coefficient between the experimental and the calculated value of the total content of carboxylate and aldehyde groups of CNFs is given for the first time.

2 Materials and Methods

2.1 Materials

Commercial microcrystalline cellulose (MCC, 15–30 μm particle size) was purchased from Nanjing Oddo Foni Biology Technology Ltd., (Nanjing, China). TEMPO was purchased from Sigma-Aldrich (Shanghai, China). Sodium periodate ($NaIO_4$), sodium bromide (NaBr), hydrochloric acid (HCl), sodium hypochlorite (NaClO), sodium hydroxide (NaOH), isopropanol ((CH_3)$_2$CHOH), and hydroxylamine hydrochloride ($NH_2OH·HCl$) were purchased from Hangzhou Mike Chemical Agents Co., Ltd., China. All chemical reagents and materials were used as received.

2.2 Chemical Treatment

The oxidation protocols are based on the previously published research [20–22]. In these studies, the dose of TEMPO is 0.5 mmol/g, while the dose of TEMPO is generally 0.1 mmol/g in the TEMPO-mediated oxidation method [23–25]. Therefore, two group of experiments with a TEMPO dose of 0.1 mmol/g were designed. The experiments were performed as shown in Tab. 1. The results of Method 3 were better than other conditions and treatments, which were reported mainly in this study.

Table 1: Experimental design

| Method | Reagent dosage (mmol/g cellulose) | | | | | |
	TEMPO	$NaIO_4$	NaBr	NaClO	Time (h)	Replication
1	0.1	2.0	8.0	8.0	4	3
2	0.1	2.5	8.0	8.0	4	3
3	0.5	2.0	8.0	8.0	9	5

First, TEMPO (0.39 g, 2.5 mmol), sodium periodate (2.14 g, 10.0 mmol), and NaBr (4.12 g, 40 mmol) were dissolved in 500 mL of distilled water with vigorous stirring. Next, 5 g microcrystalline cellulose was dispersed in the reaction mixture. Then, NaClO solution (10%, 2.7 mL, 40 mmol) was added slowly to the cellulose slurry with continuous stirring and the resulting suspension was stirred at room temperature (20–25°C) for the reaction for the designated time. The pH of the suspension was carefully maintained at about 10.5 through the addition of 2 M aqueous NaOH. During the reaction, the reaction beakers were covered with aluminum foil to prevent the photo-induced decomposition of periodate. Finally, the oxidation reaction was terminated by adding 5 mL of ethanol after the designated reaction time was reached.

The reaction slurry was separated by centrifugation at 900 g for 2 min (TD5B, Changsha Yingtai Instrument Co., Ltd., Changsha, China), the supernatant was precipitated with 1.2 times ethanol, and the formed precipitate was collected by centrifugation at 8500 g for 5 min (TG5B, Changsha Yingtai

Instrument Co., Ltd., Changsha, China). The oxidized cellulose was then washed and centrifuged several times with 95% ethanol and 0.5 M aqueous HCl. Finally, the precipitate was dispersed in water, collected by vacuum filtration, and the solid fraction was dried by vacuum freeze-drying. The powder obtained in this manner was analyzed as described below. The mass yields of the CNFs were measured as the ratio of the masses of the obtained CNFs and the cellulose initially suspended.

2.3 Determination of the Aldehyde Content

The aldehyde content of the oxidized cellulose was determined by the hydroxylamine hydrochloride (NH$_2$OH·HCl) titration method [11]. First, the oxidized cellulose of 0.1 g dry weight was dispersed into 10 mL of deionized water. Then, the 10 mL suspension of oxidized cellulose was mixed with 20 mL isopropanol, and the mixture was sufficiently stirred to form a well-dispersed slurry. Next, the pH of the mixture was adjusted to 2–3 by adding a few drops of 0.5 M hydrochloric acid and then carefully adjusted to 3.5 by the addition of 0.1 N sodium hydroxide. Fourth, 10 mL of 10 wt% hydroxylamine hydrochloride solution was added to this mixture and allowed to react for 10 min. Finally, the hydrochloric acid released from the reaction was titrated with 0.5 N sodium hydroxide solution until the pH was regained at 3.5. The aldehyde content was calculated by the following Eq. (1):

$$A_{ald} = \frac{V_{NaOH} \times \mathrm{M}}{W_{CEL}} \tag{1}$$

where A_{ald} is the content of aldehyde group in the oxidized cellulose (mmol/g); V_{NaOH} is the volume of NaOH (mL) consumed in the titration, M is the normality of the NaOH, and W_{CEL} is the dry basis weight of oxidized cellulose (g) initially dispersed.

2.4 Determination of the Carboxylate Content

The carboxylate content of each sample was determined with the conductometric titration method [20]. First, the oxidized cellulose fibers 0.1 g (dry basis) were dispersed into 0.5 M aqueous NaCl (100 mL), after which a solution of 0.1 M HCl and 0.5 M NaCl (5 mL) was slowly dropped into the dispersion, and the suspension was gently stirred. The NaOH/NaCl solution (0.1 M NaOH–0.5 M NaCl) was used for titration with a conductivity titrator (INESA ZD-2, China). The carboxylate content was calculated using the following Eq. (2):

$$[COO^-] = \frac{\left(V_{NaOH(added)} - V_{HCL}\right) \times M_{NaOH}}{W_{CEL}} \tag{2}$$

where $[COO^-]$ is the carboxylate content (mmol/g$_{cellulose}$); $V_{NaOH\ (added)}$ is the consumed volume of NaOH solution (mL) at the equivalent point; V_{HCl} is the volume of HCl added to the 0.1 M HCl–0.5 M NaCl mixed solution (mL); M_{NaOH} is the molarity of NaOH (mol/L) and W_{CEL} is the dry basis weight of oxidized cellulose (g) initially dispersed.

2.5 Fourier-Transform Infrared Spectroscopy

FTIR spectra of samples were collected with a Nicolet Magna 560 instrument (Thermo Fisher, Waltham, MA, USA) fitted with a diamond attenuated-total-reflectance (ATR) attachment. Solid samples were placed directly on the ATR crystal, and all the spectra of measured samples were recorded in ATR mode over the 500–4000 cm^{-1} range in absorbance mode, with 32 scans per spectrum at a resolution of 4 cm^{-1}. The most representative spectra of CNFs were presented.

2.6 X-Ray Diffraction

The crystallinity of MCC and the cellulose after multi-site regioselective oxidation was analyzed by X-ray diffraction (XRD). The XRD profiles were recorded by a D/max 2200 diffractometer (Rigaku, Japan) equipped with a CuKα radiation source (λ = 0.154 nm). Measurement data were collected in the diffraction 2θ angle range of 5–40° at a scanning speed of 4° min^{-1}. The crystallinity index (CrI) of samples was evaluated using the Segal method [26] according to following Eq. (3):

$$CrI\ (\%) = \frac{I_{002} - I_{am}}{I_{002}} \times 100 \tag{3}$$

where I_{002} and I_{am} represent the maximum and minimum peak intensity at around 22–23° and 18–20°, respectively.

2.7 Transmission-Electron Microscopy

Drops of dilute CNF suspensions were placed on the carbon-coated electron-microscopy grids. The excess liquid was absorbed with a piece of filter paper. Then, 1 wt% phosphotungstic acid solution was added to negatively stain the samples for about 1 minute to enhance image contrast. The excess was absorbed by filter paper. After drying, the sample grid was observed using a JEM-2100 transmission-electron microscope (JEOL Ltd., Japan) at an accelerator voltage of 200 kV. The dimensions of the CNFs were determined from the TEM images with the Image J software.

3 Results and Discussion

3.1 Spectroscopic Analyses

The FTIR technique can be used to straightforwardly evaluate the structural changes that have occurred in cellulose after multi-site regioselective oxidation. Fig. 1 displays the FTIR spectra of the MCC and CNFs prepared by Method 3. Fig. 1a displays the entire spectral region, while Fig. 1b shows an enlargement of the 1650–1750 cm^{-1} region. In the spectra of all samples, the characteristic peaks of cellulose, hydrogen-bonded
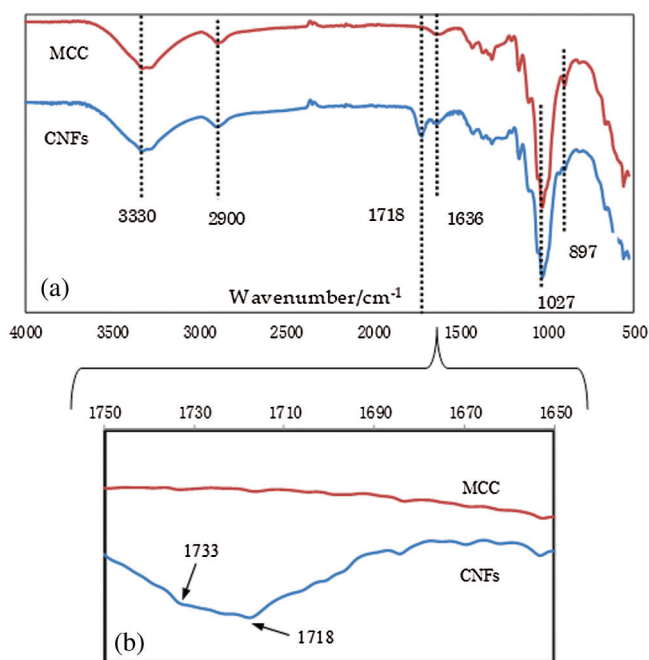

Figure 1: FTIR spectra of the MCC and CNFs prepared by Method 3

O–H stretching peak and sp^3-hybridized C–H stretching peak, appears near 3330 cm^{-1} and 2900 cm^{-1}, respectively. The shoulder observed at 1733 cm^{-1} is attributed to the carbonyl groups (C=O) of the free carboxylic groups, whereas the large sharp absorption band at 1718 cm^{-1} is assigned to the C=O stretching vibrations of the aldehyde groups [20,27]. Its asymmetry suggests the presence of overlapping peaks. The sharp absorptions at 1027 cm^{-1} are corresponded to C−O stretching [28,29], and the small peaks at 897 cm^{-1} are assiged to the stretching of hemiacetal linkages [28,30]. The small peak near 1636 cm^{-1} is attributed to the bending vibrations of residual water molecules in the MCC and CNF samples [31,32].

3.2 The Effect of Multi-Site Regioselective Oxidation on the Crystal Structure of Cellulose

To investigate the influence of the multi-site regioselective oxidation process on the crystal structure of cellulose, the XRD patterns of MCC and the CNFs prepared by Method 3 were examined (Fig. 2). The XRD pattern of each material exhibited peaks at 2θ values of around 16.5° and 22.5°, which are consistent with typical cellulose I structures [33,34], indicating that crystal integrity was maintained during the oxidation process. The crystallinities (CrI) of the original untreated MCC and the CNFs prepared through multi-site regioselective oxidation were 76.6% and 71.3%, respectively. The decrease in crystallinity is ascribed to the degradation of cellulose, but the change is ignorable.
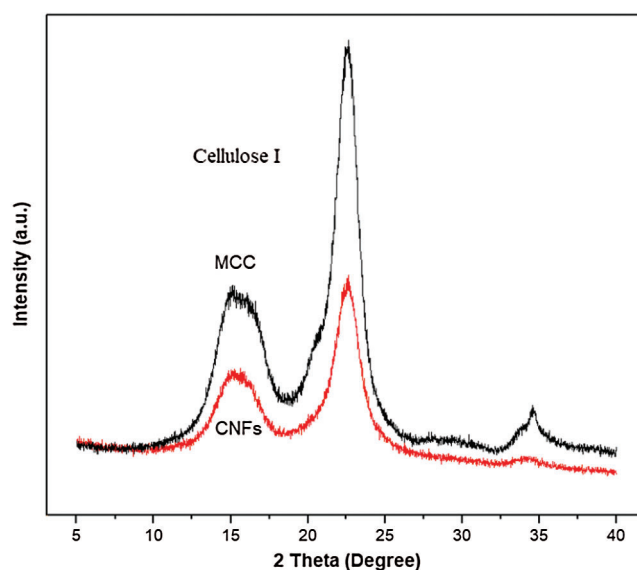

Figure 2: X-ray diffraction patterns of the MCC and CNFs prepared by Method 3

3.3 Cellulose Nanofibrils Morphology

Transmission electron microscopy revealed that the CNFs had widths below 100 nm with the average widths of 81.9, 55.4, and 14.1 nm for Method 1–3 used in this study. The TEM images of different CNFs prepared by periodate oxidation, TEMPO-periodate oxidation and TEMPO-mediated oxidation were shown Fig. 3. The periodate oxidation system selectively oxidizes the hydroxyl groups at C2 and C3 on the cellulose chain to carboxyl groups. The amorphous region of cellulose is first attacked, then the reaction occurs on the surface of the crystalline region and the ends of crystals, and then penetrates from the surface to the interior of the crystalline region [37,38]. The short-rod shape CNFs with an average width of 5–10 nm and several hundred nm in length can be prepared by periodate oxidation system (Fig. 3a) [35,37]. Since TEMPO-mediated oxidation system selectively oxidizes the C6 primary hydroxyl groups exposed on the cellulose fibril surfaces to carboxyl groups, and the crystalline core is not altered by the oxidation [23,36]. Therefore, the individual CNFs with an average width of 3–5 nm and a length
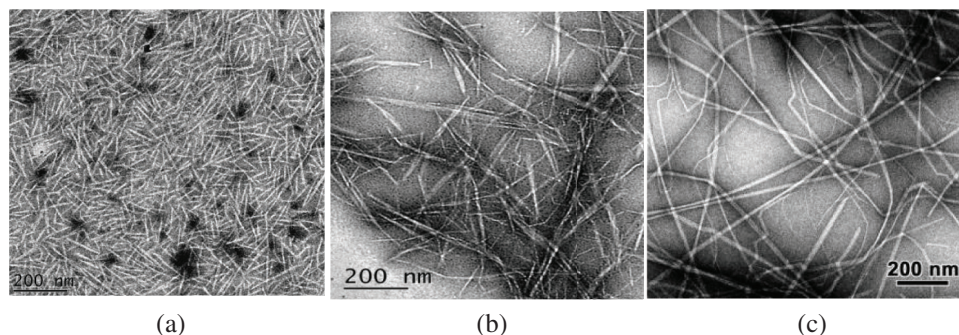
Figure 3: Transmission-electron microscopy (TEM) images of different CNFs: (a) CNFs prepared by periodate oxidation [35]; (b) CNFs prepared by TEMPO-periodate oxidation in this study; (c) CNFs prepared by TEMPO-mediated oxidation [36], reproduction of the image with permission from American Chemical Society. (a) Periodate oxidation. (b)TEMPO-periodate oxidation. (c)TEMPO-mediated oxidation

of several μm can be prepared by TEMPO-mediated oxidation (Fig. 3c) [23,36]. As shown in Fig. 3, the morphology of CNFs prepared by multi-site regioselective oxidation (concurrent oxidation with TEMPO and periodate) are different from the former two CNFs. The particle length of CNFs prepared by the periodate oxidation method is significantly shorter than those of CNFs prepared by the TEMPO-mediated oxidation and the multi-site regioselective oxidation methods.

3.4 Theoretical Calculation of Carboxylate and Aldehyde Groups on the Surface of CNFs

The carboxylate and aldehyde contents of the CNFs were determined using titration methods, as described in Sections 2.3 and 2.4. The aldehyde-group contents of the CNFs were determined to be 0.80, 0.80 and 2.26 mmol/g, while the carboxylate contents were 0.14, 0.46, and 2.91 mmol/g for Methods 1–3 in this study.

A model was developed to calculate the total content of carboxylate and aldehyde groups of CNFs based on the microstructure model of CNFs shown in Fig. 4 [39]. The hydroxyl groups on the surface of CNFs facing the outside can be oxidized to carboxylate or aldehyde groups since the oxidation reaction of periodate and TEMPO occurs firstly on the outer surface of cellulose, and the generated carboxylate and aldehyde groups are mainly distributed on the outer surface of CNFs [28,37–39]. In addition, only half of the hydroxyl groups can be oxidized to carboxylate and aldehyde groups due to the *gt* conformation of the surface cellulose molecules [39]. The length of the cellulose basic unit cellobiose on the cellulose molecular chain is 1.03 nm [40]. Regardless of the influence of lignin and hemicellulose residues in
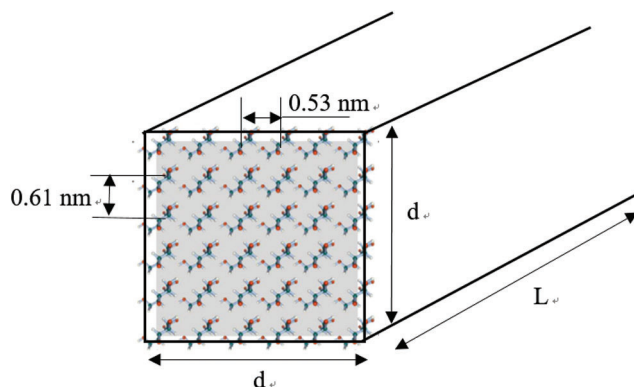

Figure 4: A microstructure model of cellulose nanofibrils used in calculation model [39]

purified cellulose, it is assumed that the CNFs is composed of a total of B cellulose molecular chains, and C cellulose molecular chains are exposed to the outside. The average width and length of CNFs was assumed to be d and L nm, respectively. The relative molecular mass of a hydroglucose ring is calculated with 162, and the Avogadro's constant is expressed by N_A.

The mass of cellulose nanofibrils of length L is given by [35]

$$\frac{L}{1.03} \times 2 \times B \times \frac{162}{N_A} = \frac{314.555LB}{N_A} \tag{4}$$

The total number of carboxylate and aldehyde groups facing the exterior is given by

For the TEMPO mediated oxidation method,

$$C \times \frac{L}{1.03} \times 2 \times \frac{1}{2} \times 1 = 0.9709LC \tag{5}$$

For the periodate oxidation method,

$$C \times \frac{L}{1.03} \times 2 \times \frac{1}{2} \times 2 = 1.9417LC \tag{6}$$

For the multi-site regioselective oxidation method or TEMPO-periodate oxidation method,

$$C \times \frac{L}{1.03} \times 2 \times \frac{1}{2} \times 3 = 2.9126LC \tag{7}$$

and the total content of carboxylate and aldehyde groups (TCA) is given by

For the TEMPO mediated oxidation method,

$$\text{TCA} = \frac{0.9709LC}{N_A} \times 10^3 \times \frac{N_A}{314.555LB} = \frac{3.0865C}{B} mmol/g \tag{8}$$

For the periodate oxidation method,

$$\text{TCA} = \frac{1.9417LC}{N_A} \times 10^3 \times \frac{N_A}{314.555LB} = \frac{6.1727C}{B} mmol/g \tag{9}$$

For the multi-site regioselective oxidation method or TEMPO-periodate oxidation method,

$$\text{TCA} = \frac{2.9126LC}{N_A} \times 10^3 \times \frac{N_A}{314.555LB} = \frac{9.2592C}{B} mmol/g \tag{10}$$

The ratio of the number (C) of cellulose molecular chains exposed to the surface to the total number (B) of molecular chains of the CNFs can be calculated using the following formula [39].

$$\frac{C}{B} = \frac{2 \times (\frac{d}{0.61} + \frac{d}{0.53})}{(\frac{d}{0.61} + 1) \times (\frac{d}{0.53} + 1)} \tag{11}$$

The total content of carboxylate and aldehyde groups on the surface of CNFs for the TEMPO mediated oxidation, the periodate oxidation, and the multi-site regioselective oxidation methods were calculated using the Eqs. (8)–(11). The results are listed in the Tab. 2.

Table 2: Total content of carboxylate and aldehyde groups on the surface of CNFs

No.	Material	Method	Reaction time (h)	Particle width (nm)	Experimental value (mmol/g)	Calculated value (mmol/g)	References
1	Softwood pulp	T	5.0	3.1	1.70	1.6199	[13]
2	Softwood pulp	T	5.0	3.1	1.80	1.6199	[41]
3	Softwood pulp	T	4.0	3.8	1.72	1.4004	[24]
4	Hardwood pulp	T	4.3	3.8	1.69	1.4004	[24]
5	Cotton	T	3.7	5.4	1.36	1.0743	[24]
6	Bacteria	T	2.7	5.8	1.15	1.0059	[24]
7	Halocynthia	T	2.5	9.1	0.65	0.6849	[24]
8	Cladophora	T	3.0	13.2	0.52	0.4916	[24]
9	Softwood pulp	I	3.0	25.0	1.75	1.0763	[15]
10	Hardwood pulp	I	3.0	25.0	1.80	1.0763	[42]
11	Rice straw	I	24.0	13.3	3.77	1.9460	[35]
12	Wheat straw	I	24.0	8.4	3.90	2.9386	[35]
13	Corn straw	I	24.0	7.9	4.04	3.0996	[35]
14	Cellulose pulp	I	42.0	8.0	8.20	3.0660	[43]
15	Softwood pulp	I	84.0	5.6	8.80	4.1407	[39]
16	MCC	I	72.0	5.0	10.97	4.5365	[44]
17	CNC	I	160.0	3.6	12.50	5.8279	[38]
18	Softwood pulp	T + I	120.0	10.0	7.20	5.6687	[27]
19	MCC	T + I	9.0	14.1	5.17	4.1413	Present study
20	MCC	T + I	4.0	55.4	1.26	1.1208	Present study
21	MCC	T + I	4.0	81.9	0.94	0.7626	Present study

MCC = Microcrystalline cellulose; CNC = Cellulose nanocrystals; T = TEMPO-mediated oxidation method; I = Periodate oxidation method; T + I = Multi-site regioselective oxidation method or TEMPO-periodate oxidation method.

As shown in Fig. 5, the calculated values have the same trend as the experimental values for the TEMPO mediated oxidation method, and the correlation coefficient (R) is 0.98. The total content of carboxylate and aldehyde groups increases as the particle width of CNFs becomes small. This is because the smaller the particle width of CNFs, the more the oxidized groups are formed on the surface of the elementary fibrils. Almost all the calculated values fall within the 95% confidence interval of the regression curve derived from the experimental values. Moreover, the type of raw materials (softwood, hardwood, cotton, bacterial, tunicate, and algal celluloses) and the reaction time (the oxidation end point from 2.5 h to 5 h) have little effect on the calculation accuracy of the model. In addition, these results also prove that the oxidation reaction of the TEMPO mediated oxidation method mainly occurs on the surface of the elementary fibrils. The CNFs retains the basic structure of elementary fibrils and is not prone to degradation reactions with TEMPO mediated oxidation. The model developed in this study can be used to calculate the total content of carboxylate and aldehyde groups of CNFs prepared by TEMPO mediated oxidation method based on the particle width.

As shown in Fig. 6, although the calculated value and the experimental value also have the same change trend for the periodate oxidation method, the experimental value and the calculated value have a large
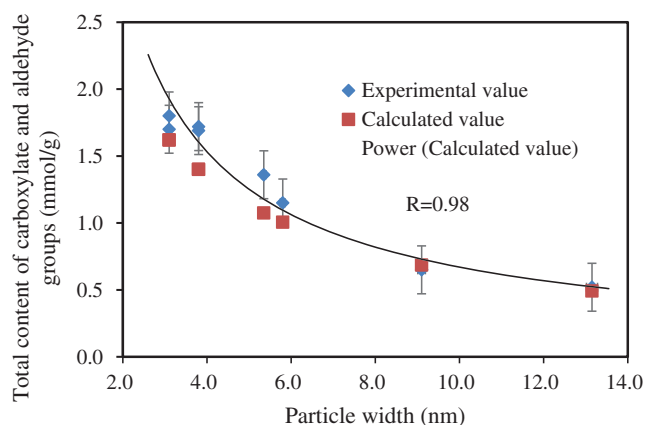
Figure 5: The relationship between total content of carboxylate and aldehyde groups and particle width for monocarboxyl CNFs (TEMPO mediated oxidation method)
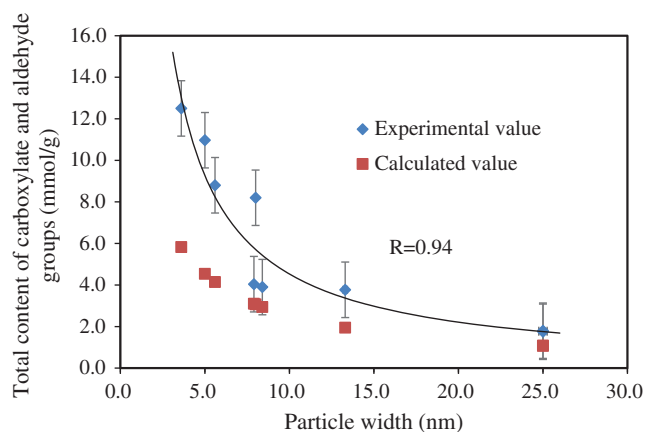

Figure 6: The relationship between total content of carboxylate and aldehyde groups and particle width for dicarboxyl CNFs (periodate oxidation method)

deviation, and the correlation coefficient (R) is 0.94. When the particle width is greater than 10 nm, the estimated value is still mostly within the 95% confidence interval of the regression curve derived from the experimental values. But when the particle width of CNFs is less than 10 nm or the oxidation time is greater than 24 h, the experimental value is much larger than the calculated value. This may be explained as follows. Because the periodate is a strong oxidant, the oxidation reaction of cellulose not only occurs on the surface of the microfibrils, but also proceeds to the inside of the microfibrils when the reaction proceeds to a certain time [37,38]. Fig. 3 also shows that the length of CNFs prepared by the periodate oxidation method is significantly shorter than those of CNFs prepared by the TEMPO-mediated oxidation and the multi-site regioselective oxidation methods. After the structure of the elementary fibrils is destroyed, the cellulose undergoes peroxidative degradation and the cellulose molecular chain is also destroyed. A large number of functional groups are formed, resulting in an increase in the total content of carboxylate and aldehyde groups. Therefore, the model developed in this study is not suitable to calculate the total content of carboxylate and aldehyde groups of CNFs prepared by the periodate oxidation method based on the particle width.

As shown in Fig. 7, the calculated value has the same trend as the experimental value for the multi-site regioselective oxidation method, and the correlation coefficient (R) is 0.99. Almost all the calculated values
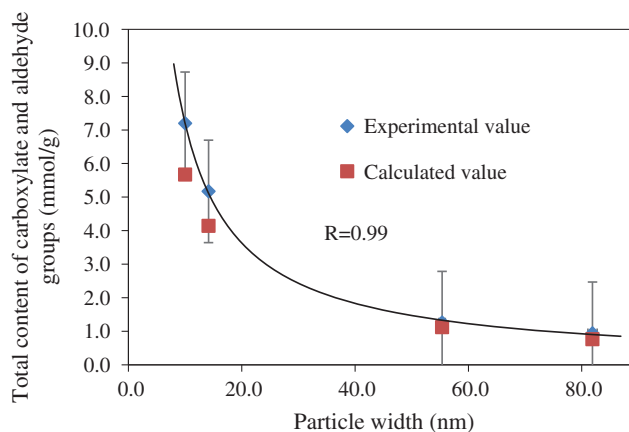
Figure 7: The relationship between total content of carboxylate and aldehyde groups and particle width for tricarboxyl CNFs (multi-site regioselective oxidation method)

fall within the 95% confidence interval of the regression curve derived from the experimental values. The results show that the model can be used to calculate the total content of carboxylate and aldehyde groups of CNFs prepared by the multi-site regioselective oxidation method.

3.5 CNFs Yield

The CNFs yields of the Methods 1 and 2 were not more than 5%. The reason may be that the TEMPO dose is too small or the reaction time is too short. The CNFs yield of the Method 3 was $20.2 \pm 1.5\%$ (n = 5). This yield is still lower than those of the TEMPO-mediate oxidation method or the periodate oxidation method [14,35]. This is because part of the CNFs was mixed into the precipitation during the centrifugal separation of the reaction slurry. The yields are expected to increase by improving the separation method or optimizing the reaction processes in the future.

4 Conclusions

CNFs were prepared through the multi-site regioselective oxidation of microcrystalline cellulose with TEMPO and periodate. Transmission electron microscopy revealed that the CNFs had the average widths of 14.1, 55.4, and 81.9 nm for three different treatments. FTIR spectroscopy revealed the formation of carboxyl groups on the surfaces of the microfibrils. XRD studies of the treated and untreated cellulose fibers showed that, not only was the cellulose I structure maintained during oxidation, but the crystallinity index of the CNFs produced in this manner exceeded 70% for all samples. The results demonstrate that CNFs can be prepared by multi-site regioselective oxidation. In addition, a model was developed to calculate the total content of carboxylate and aldehyde groups of CNFs prepared by the TEMPO mediate oxidation, the periodate oxidation and the multi-site regioselective oxidation methods based on the particle width of CNFs. The calculated values of the model were in good agreement with the total content (experimental value) of carboxylate and aldehyde groups of CNFs prepared by the TEMPO-mediated oxidation and the multi-site regioselective oxidation methods. The correlation coefficients of the calculated values and the experimental values for the TEMPO mediate oxidation and the multi-site regioselective oxidation methods were 0.98 and 0.99, respectively. The model was not valid for CNFs prepared by the periodate oxidation system. These results will help the expert to easier know the oxidation level of cellulose based on the particle width of CNFs.

Conflicts of Interest: The authors declare that they have no conflicts of interest to report regarding the present study.

References

1. Klemm, D., Kramer, F., Moritz, S., Lindstrom, T., Ankerfors, M. et al. (2011). Nanocelluloses: a new family of nature-based materials. *Angewandte Chemie International Edition, 50(24),* 5438–5466. DOI 10.1002/anie.201001273.

2. Sun, X. Z., Moon, D., Yagishita, T., Minowa, T. (2013). Evaluation of energy consumption and greenhouse gas emissions in preparation of cellulose nanofibers from woody biomass. *Transactions of the ASABE, 56,* 1061–1067.

3. Dufresne, A. (2013). Nanocellulose: a new ageless bionanomaterial. *Materials Today, 16(6),* 220–227. DOI 10.1016/j.mattod.2013.06.004.

4. Jarvis, M. (2003). Chemistry: cellulose stacks up. *Nature, 426(6967),* 611–612. DOI 10.1038/426611a.

5. Somerville, C., Bauer, S., Brininstool, G., Facette, M., Hamann, T. et al. (2004). Toward a systems approach to understanding plant cell walls. *Science, 306(5705),* 2206–2208. DOI 10.1126/science.1102765.

6. Qing, Y., Sabo, R., Zhu, J. Y., Agarwal, U., Cai, Z. et al. (2013). A comparative study of cellulose nanofibrils disintegrated via multiple processing approaches. *Carbohydrate Polymers, 97(1),* 226–234. DOI 10.1016/j.carbpol.2013.04.086.

7. Ferrer, A., Filpponen, I., Rodríguez, A., Laine, J., Rojas, O. J. (2012). Valorization of residual Empty Palm Fruit Bunch Fibers (EPFBF) by microfluidization: production of nanofibrillated cellulose and EPFBF nanopaper. *Bioresource Technology, 125,* 249–255. DOI 10.1016/j.biortech.2012.08.108.

8. Abe, K., Yano, H. (2009). Comparison of the characteristics of cellulose microfibril aggregates of wood, rice straw and potato tuber. *Cellulose, 16(6),* 1017–1023. DOI 10.1007/s10570-009-9334-9.

9. Abdul Khalil, H. P. S., Davoudpour, Y., Islam, M. N., Mustapha, A., Sudesh, K. et al. (2014). Production and modification of nanofibrillated cellulose using various mechanical processes: a review. *Carbohydrate Polymers, 99,* 649–665. DOI 10.1016/j.carbpol.2013.08.069.

10. Keckes, J., Burgert, I., Frühmann, K., Müller, M., Kölln, K. et al. (2003). Cell-wall recovery after irreversible deformation of wood. *Nature Materials, 2(12),* 810–814. DOI 10.1038/nmat1019.

11. Tejado, A., Alam, M. N., Antal, M., Yang, H., van de Ven, T. G. M. (2012). Energy requirements for the disintegration of cellulose fibers into cellulose nanofibers. *Cellulose, 19(3),* 831–842. DOI 10.1007/s10570-012-9694-4.

12. Dong, S., Bortner, M. J., Roman, M. (2016). Analysis of the sulfuric acid hydrolysis of wood pulp for cellulose nanocrystal production: a central composite design study. *Industrial Crops and Products, 93,* 76–87. DOI 10.1016/j.indcrop.2016.01.048.

13. Isogai, A., Saito, T., Fukuzumi, H. (2011). TEMPO-oxidized cellulose nanofibers. *Nanoscale, 3(1),* 71–85. DOI 10.1039/C0NR00583E.

14. Isogai, A., Hänninen, T., Fujisawa, S., Saito, T. (2018). Catalytic oxidation of cellulose with nitroxyl radicals under aqueous conditions. *Progress in Polymer Science, 86,* 122–148. DOI 10.1016/j.progpolymsci.2018.07.007.

15. Liimatainen, H., Visanko, M., Sirvio, J. A., Hormi, O. E., Niinimaki, J. (2012). Enhancement of the nanofibrillation of wood cellulose through sequential periodate-chlorite oxidation. *Biomacromolecules, 13(5),* 1592–1597. DOI 10.1021/bm300319m.

16. Abitbol, T., Kloser, E., Gray, D. G. (2013). Estimation of the surface sulfur content of cellulose nanocrystals prepared by sulfuric acid hydrolysis. *Cellulose, 20(2),* 785–794. DOI 10.1007/s10570-013-9871-0.

17. Salminen, R., Reza, M., Pääkkönen, T., Peyre, J., Kontturi, E. (2017). TEMPO-mediated oxidation of microcrystalline cellulose: limiting factors for cellulose nanocrystal yield. *Cellulose, 24(4),* 1657–1667. DOI 10.1007/s10570-017-1228-7.

18. Wei, J., Chen, Y., Liu, H., Du, C., Yu, H. et al. (2016). Effect of surface charge content in the TEMPO-oxidized cellulose nanofibers on morphologies and properties of poly(N-isopropylacrylamide)-based composite hydrogels. *Industrial Crops and Products, 92,* 227–235. DOI 10.1016/j.indcrop.2016.08.006.

19. Sun, X. Z., Song, L. Y., Pei, X. X. (2018). Method for preparing nanocrystalline cellulose by multi-site oxidation method, and application thereof.

20. Coseri, S., Biliuta, G., Zemljic, L., Srndovic, J., Larsson, P. T. et al. (2015). One-shot carboxylation of microcrystalline cellulose in the presence of nitroxyl radicals and sodium periodate. *RSC Advances, 5(104),* 85889–85897. DOI 10.1039/C5RA16183E.

21. Mendoza, D. J., Browne, C., Raghuwanshi, V. S., Simon, G. P., Garnier, G. (2019). One-shot TEMPO-periodate oxidation of native cellulose. *Carbohydrate Polymers, 226,* 115292. DOI 10.1016/j.carbpol.2019.115292.

22. Baron, R. I., Bercea, M., Avadanei, M., Lisa, G., Biliuta, G. et al. (2019). Green route for the fabrication of self-healable hydrogels based on tricarboxy cellulose and poly(vinyl alcohol). *International Journal of Biological Macromolecules, 123,* 744–751. DOI 10.1016/j.ijbiomac.2018.11.107.

23. Saito, T., Hirota, M., Tamura, N., Kimura, S., Fukuzumi, H. et al. (2009). Individualization of Nano-sized plant cellulose fibrils by direct surface carboxylation using TEMPO catalyst under neutral conditions. *Biomacromolecules, 10(7),* 1992–1996. DOI 10.1021/bm900414t.

24. Okita, Y., Saito, T., Isogai, A. (2010). Entire surface oxidation of various cellulose microfibrils by TEMPO-Mediated oxidation. *Biomacromolecules, 11(6),* 1696–1700. DOI 10.1021/bm100214b.

25. Kuramae, R., Saito, T., Isogai, A. (2014). TEMPO-oxidized cellulose nanofibrils prepared from various plant holocelluloses. *Reactive & Functional Polymers, 85,* 126–133. DOI 10.1016/j.reactfunctpolym.2014.06.011.

26. Segal, L., Creely, J. J., Martin, J. A. A., Conrad, C. M. (1959). An empirical method for estimating the degree of crystallinity of native cellulose using the X-ray diffractometer. *Textile Research Journal, 29(10),* 786–794. DOI 10.1177/004051755902901003.

27. Yang, H., Tejado, A., Alam, N., Antal, M., van de Ven, T. G. M. et al. (2012). Films prepared from electrosterically stabilized nanocrystalline cellulose. *Langmuir, 28(20),* 7834–7842. DOI 10.1021/la2049663.

28. Errokh, A., Magnin, A., Putaux, J. L., Boufi, S. (2018). Morphology of the nanocellulose produced by periodate oxidation and reductive treatment of cellulose fibers. *Cellulose, 25(7),* 3899–3911. DOI 10.1007/s10570-018-1871-7.

29. Garcia, A., Labidi, J., Belgacem, M. N., Bras, J. (2017). The nanocellulose biorefinery: woody versus herbaceous agricultural wastes for NCC production. *Cellulose, 24(2),* 693–704. DOI 10.1007/s10570-016-1144-2.

30. Kim, U. J., Kuga, S., Wada, M., Okano, T., Kondo, T. (2000). Periodate oxidation of crystalline cellulose. *Biomacromolecules, 1(3),* 488–492. DOI 10.1021/bm0000337.

31. Fukuzumi, H. (2012). *Studies on structures and properties of TEMPO-oxidized cellulose nanofibril films (Ph.D. Thesis).* The University of Tokyo, Japan.

32. Johar, N., Ahmad, I., Dufresne, A. (2012). Extraction, preparation and characterization of cellulose fibres and nanocrystals from rice husk. *Industrial Crops and Products, 37(1),* 93–99. DOI 10.1016/j.indcrop.2011.12.016.

33. Nishiyama, Y., Langan, P., Chanzy, H. (2002). Crystal structure and hydrogen bonding system in cellulose I from synchrotron X-ray and neutron fiber diffraction. *Journal of the American Chemical Society, 124(31),* 9074–9082. DOI 10.1021/ja0257319.

34. Nishiyama, Y., Sugiyama, J., Chanzy, H., Langan, P. (2003). Crystal structure and hydrogen bonding system in cellulose Iα from synchrotron X-ray and neutron fiber diffraction. *Journal of the American Chemical Society, 125(47),* 14300–14306. DOI 10.1021/ja037055w.

35. Sun, X. Z., He, Q., Yang, Y. (2020). Preparation of dicarboxyl cellulose nanocrystals from agricultural wastes by sequential periodate-chlorite oxidation. *Journal of Renewable Materials, 8(4),* 447–460. DOI 10.32604/jrm.2020.09671.

36. Saito, T., Nishiyama, Y., Putaux, J. L., Vignon, M., Isogai, A. (2006). Homogeneous suspensions of individualized microfibrils from TEMPO-catalyzed oxidation of native cellulose. *Biomacromolecules, 7(6),* 1687–1691. DOI 10.1021/bm060154s.

37. Chen, D., van de Ven, T. G. M. (2016). Morphological changes of sterically stabilized nanocrystalline cellulose after periodate oxidation. *Cellulose, 23(2),* 1051–1059. DOI 10.1007/s10570-016-0862-9.

38. Conley, K., Whitehead, M. A., van de Ven, T. G. M. (2016). Chemically peeling layers of cellulose nanocrystals by periodate and chlorite oxidation. *Cellulose, 23(3),* 1553–1563. DOI 10.1007/s10570-016-0922-1.

39. Funahashi, R., Okita, Y., Hondo, H., Zhao, M., Saito, T. et al. (2017). Different conformations of surface cellulose molecules in native cellulose microfibrils revealed by layer-by-layer peeling. *Biomacromolecules, 18(11),* 3687–3694. DOI 10.1021/acs.biomac.7b01173.

40. Stone, B. (2005). Cellulose: structure and distribution. In: *Encyclopedia of Life Sciences: Plant Science- Plant Cell Growth.* New York: John Wiley & Sons. DOI 10.1038/npg.els.0003892.

41. Tanaka, R., Saito, T., Ishii, D., Isogai, A. (2014). Determination of nanocellulose fibril length by shear viscosity measurement. *Cellulose, 21(3),* 1581–1589. DOI 10.1007/s10570-014-0196-4.

42. Kekalainen, K., Liimatainen, H., Niinimaki, J. (2014). Disintegration of periodate-chlorite oxidized hardwood pulp fibers to cellulose mocrofibrils: kinetics and charge threshold. *Cellulose, 21(5),* 3691–3700. DOI 10.1007/s10570-014-0363-7.

43. Yang, H., Chen, D., van de Ven, T. G. M. (2015). Preparation and characterization of sterically stabilized nanocrystalline cellulose obtained by periodate oxidation of cellulose fibers. *Cellulose, 22(3),* 1743–1752. DOI 10.1007/s10570-015-0584-4.

44. Munster, L., Vicha, J., Klofac, J., Masar, M., Kucharczyk, P. et al. (2017). Stability and aging of solubilized dialdehyde cellulose. *Cellulose, 24(7),* 2753–2766. DOI 10.1007/s10570-017-1314-x.